Biofunctionalised Patterned Polymer Brushes via Thiol-Ene Coupling for the Control of Cell Adhesion and the Formation of Cell Arrays

Burcu Colak,[1,2] Stefania Di Cio[1,2] and Julien E. Gautrot[1,2]*

[1] Institute of Bioengineering and [2] School of Engineering and Materials Science, Queen Mary, University of London, Mile End Road, London, E1 4NS, UK.

* To whom correspondence should be addressed E-mail: j.gautrot@qmul.ac.uk.

Abstract

Thiol-ene radical coupling is increasingly used for the biofunctionalisation of biomaterials. Thiol-ene chemistry presents interesting features that are particularly attractive for platforms requiring specific reactions with peptides or proteins and the patterning of cells, such as reactivity in physiological conditions and photo-activation. In this work, we synthesised alkene-functionalised (allyl and norbornene residues) anti-fouling polymer brushes (based on poly(oligoethyleneglycol methacrylate)) and studied thiol-ene coupling with a series of thiols including cell adhesive peptides RGD and REDV. The adhesion of human umbilical vein endothelial cells human umbilical vein endothelial cells (HUVECs) to these interfaces was studied and highlighted the absence of specific integrin engagement to REDV, in contrast to the high level of cell spreading observed on RGD-functionalised polymer brushes. This revealed that $\alpha_4\beta_1$ integrins (binding to REDV sequences) are not sufficient on their own to sustain HUVEC spreading, in contrast to $\alpha_v\beta_3$ and $\alpha_5\beta_1$ integrins. In addition, we photopatterned peptides at the surface of poly (oligoethylene glycol methacrylate) (POEGMA)

brushes and characterised the quality of the resulting arrays by epifluorescence microscopy and atomic force microscopy (AFM). This allowed the formation of cell patterns and demonstrated the potential of thiol-ene based photopatterning for the design of cell microarrays.

Introduction

The control and manipulation of interfaces between materials and biological systems is particularly important for the development of biomedical applications such as tissue engineering and in vitro cell-based assays. Surface engineering using polymer coatings has proved very successful for the control of hydrophilicity, surface charge, chemical reactivity, protein resistance, adhesion, mechanics and topography.[1-6] In particular, recent advances in patterning technologies have allowed the precise patterning of cells and cell colonies, therefore enabling unprecedented control of single cell and cell cluster shape and organisation or migration.[7-14] Indeed extra-cellular matrix (ECM) protein micropatterns have been developed to control cell spreading and shape and how such geometrical cues regulate cell phenotype.[15, 16] In the case of mesenchymal stem cells and epidermal stem cells, changes in cytoskeleton organisation, guided by the geometry of the ECM, regulate differentiation[15, 16] and the compartmentatlisation of stem cell clusters.[10]

For such applications, polymer coatings should allow a precise control of protein adsorption and integrin binding. In this respect, polymer brushes are particularly well-suited as they can be design with a wealth of chemical functionalities and enable the attachment and immobilisation of biomolecules.[17, 18] In particular, polymer brushes based on oligo(ethylene glycol methacrylate) (OEGMA), carboxybetaine methacrylamide and hydroxypropyl methacrylamide display exceptional protein resistance, even in the presence of complex protein solutions such as serum (relevant to cell culture), plasma and blood.[9, 19-23] Therefore such

brushes have been patterned using micro-contact printing (μCP)[9, 19] and, more recently electrospun fibre nanolithography[24] (ENL) to define nano- to micro-scale ECM protein patterns that can regulate cell adhesion and spreading. In this respect, the excellent prolonged protein resistance of polymer brushes such as POEGMA, even in tissue culture conditions, is particularly attractive for cell-based assays requiring several days of culture.[9] In addition, the ease with which polymer brushes with a wide range of chemistries can be patterned is attractive to study the synergistic roles of ECM geometry and matrix physico-chemical properties on cell adhesion, spreading and phenotype.[25]

The biofunctionalistion of polymer brushes has also attracted considerable interest, from the immobilisation of enzymes[26-28] to the development of biosensors.[21, 29, 30] In particular, peptides have been coupled to polymer brushes through a range of strategies,[31-35] to confer biospecificity to antifouling polymer brushes such as POEGMA. This strategy proved very successful for the control of cell adhesion and the study of the synergistic binding of different integrin ligands as well as their 3D spatial localisation.[36, 37] However, to date few polymer brush-based interfaces have been micropatterned with peptides to enable the simultaneous control of cell shape and the binding of specific integrins[35] and parameters controlling suitable biofunctionalisation strategies and patterning fidelity remain largely unexplored.

In the present work, we report the functionalisation of POEGMA brushes with peptides, via thiol-ene chemistry. Radical mediated thiol-ene coupling has attracted attention from the biomaterials community owing to its efficiency in mild conditions, including at physiological pH, buffer and ionic strength.[14, 38-40] In addition, peptides are attractive candidates used for biofunctionalisation via thiol-ene coupling as they can be designed to present cysteine residues relatively readily.[41-43] Maleimide-based Michael addition has been used to promote the coupling of antibacterial peptides[32, 33, 44] to polymer brushes, but few works have focused on

the radical-based tethering of thiols to brushes[14, 35], in particular those displaying antifouling properties. Previous work in this area focused on the use of allylamine-functionalised poly(glycidyl methacrylate) brushes to promote thiol-ene coupling[35], however these substrates are poorly adapted for the specific control of cell adhesion as the resulting coatings are too hydrophobic and positively charged. We proposed to simply functionalise hydroxyl-terminated POEGMA brushes (POEGMA-OH) with alkenes that can sustain thiol-ene coupling. We characterised the efficiency of POEGMA brush functionalisation with a range of thiols, including peptides. We then studied cell adhesion to the resulting biofunctionalised brushes, with the aim to characterise the specificity of the peptides tethered to promote integrin binding in human umbilical vein endothelial cells (HUVECs). In addition we used thiol-ene coupling of labelled peptides to characterise the quality of peptide patterns generated via photo-irradiation through masks, and demonstrated the design of cellular microarrays using this approach.

Materials and methods

Materials

Anhydrous toluene (99.8 %), triethylamine (99 %), ethanol (99.5 %), 3-(trimethoxysilyl)propyl methacrylate (98%), methanol (99.9 %), phosphate buffer saline (PBS) tablets, Dulbecco's PBS, poly (ethylene glycol) methacrylate average Mn 360 (409537), bipyridine (99 %), copper (II) bromide (99.999 %), copper (I) chloride (99.995 %), disuccinimyl carbonate (DSC) (95 %), 4-dimethylaminopyridine (DMAP) (99 %), dimethylformamide (DMF) (pharmaceutical secondary standard), allylamine (98 %), hexamethylenediamine (98 %) triethanolamine (99 %), Eosin Y (99 %), IRG2959 (98 %), N-acetyl L-cysteine (**T1**, 99%), L-glutathione reduced (**T2**, 98 %), paraformaldehyde (PFA) (95 %), Triton-X 100, phalloidin–tetramethylrhodamine

B isothiocyanate and DAPI (98 %) were obtained from Sigma Aldrich. Atom-transfer radical polymerisation (ATRP) silane initiator, 3-trimethoxysilyl propyl 2-bromo-2 methylpropionate was purchased from Fluorochem. Medium 199, 2-{4-(2-hydroxyethyl)piperazin-1-yl]ethanesulfonic acid (HEPES) was purchased from life technologies. Collagen rat type I was purchased from BD Biosciences. Custom peptides (> 95% purity, high-performance liquid chromatography (HPLC) GCGREDVSG (**T3**, REDV), GCGRVDESG (**T4**, RDVE), GCGYGRGDSPG (**T5**, RGD), GCGYGRGESPG (**T6**, RGE), GCGPHSRNSG (**T7**, PHSRN), GCGYGRGESPG-Lys-FITC-G (**T8**, FITC-RGE) were purchased from Proteogenix, France. Penicillin streptomycin (5000 U/mL) and medium 199 HEPES (22340020) were obtained from life technologies. Fetal bovine serum (FBS), South American Origin was purchased from Labtech. (Endo-cis-5-norbornene-2,3- dicarboxylic anhydride) (99 %), L-glutamine (200 mM), versene and trypsin (0.25 %) phenol red, were obtained from Thermo Fisher Scientific.

Instrumentation

Dry brush thicknesses were measured via ellipsometry, using an α-SE ellipsometer from J.A. Woolam Co., Inc. Ellipsometry solutions. For in situ measurements, in deionised water, substrates were placed in chamber fitted with quartz windows normal to the incident beam path. The refractive index of the medium was obtained using data recorded for bare silicon substrate in deionised water. Measurements were carried out in triplicate.Grazing angle fourier-transform infrared spectroscopy (FTIR) was carried out using a Bruker Tensor 27 spectrometer equipped with a MCT detector; results were acquired at a resolution of 16 cm^{-1} and a total of 128 scans per run in the region of 600-4000 cm^{-1}. ^{1}H nuclear magnetic resonance (NMR) and ^{13}C NMR spectroscopy was produced using Bruker AV 400. Mass spectrometry was carried out using an Agilent Technologies 1100 series equipped with a LC/MSD trap. XPS was measured using thermo K-Alpha XPS system. The ultraviolet (UV) light used to initiate reactions was the Omnicure series 1500. The radiometer used to measure the UV light intensity

was from International light technologies, ILT 1400-A radiometer photometer. The visible light used to initiate the reaction was generated using an OSL2 fibre illuminator from Thorlabs. AFM was used to scan surfaces, in semicontact mode and the row pictures were corrected with a first order function using Nova software. Non-contact NSG01 cantilevers from NT-MDT were used (force constant 1,45-15,1 N/m and resonant frequency 87-230 kHz). A Leica DMI4000B epifluorescence microscope fitted with a HCX PL FLUOTAR 10x/0.3 PJ1 objective and a Leica DFC300 FX CCD camera was used to image patterned surfaces. Analysis of microscopy images was carried out using Image J; singe channel images were changed to grey scale then to black and white using a threshold (with cells appearing black), binary watershedding was performed to identify individual cells.

Calculation of functionalisation levels from ellipsometry data

As described in a previous report[35], polymer brush funcationalisation levels were calculated according to:

$$\Delta T = Tn - Ti \qquad \textbf{Equation 1}$$

Where ΔT is the difference in dry brush thickness (in nm) between Tn (new dry brush thickness after functionalisation) and Ti (initial dry brush thickness). The degree of functionalisation (in %) fn is obtained according to:

$$fn = \left(\frac{\Delta T}{Ti} \times \frac{M1}{M2}\right) \times 100 \qquad \textbf{Equation 2}$$

Where M1 and M2 are the molecular weight of initial repeat units and that of the added fragments (in g/mol).

Statistical analysis

All data were analysed by Tukey's test and significance was determined by * $p < 0.05$, ** $p < 0.01$: *** $p < 0.001$. A full summary of statistical analysis is provided in Supplementary Tables S1 to S6.

*Synthesis of norbornene derivative **1***

A hexamethylenediamine solution (6.5 wt%) in tetrahydrofuran and water (2.5:1) was prepared. Separately, (endo-cis-5-norbornene-2,3- dicarboxylic anhydride) (5 wt%) was dissolved in tetrahydrofuran. The (endo-cis-5-norbornene-2,3- dicarboxylic anhydride) solution was slowly added to the hexamethylenediamine solution and the mixture was heated to 50 °C for 1 h. The mixture was recrystallised in tetrahydrofuran containing a small quantity of water. The crystals were filtered, washed with tetrahydrofuran and dried under reduced pressure. Melting point 152 °C, m/z 279 (M-; expected 279). See Supplementary Figure S13 for spectrum. δ_H (400 MHz; D_2O) 1.2-1.4 (8H, m), 1.6 (2H, m), 2.9-3.1 (6H, m), 3.15 (2H, m), 6.0 (1H, m) and 6.3 (1H, m). δ_C (400MHz, D_2O) 180.9, 175.9, 136.8, 133.8, 52.8, 49.8, 49.1, 46.8, 46.3, 39.3, 39.0, 28.0, 27.9, 25.4, 25.0. v/cm^{-1} 3231 (N-H, w), 3000-2500 (O-H, br), 2934-2861 (C-H, w), 1688 (C=O carboxylic acid, m), 1633 (C=O amide, s), 1549 (N-H, C-N, s), 1392 (C-O, s), 1290 (C-N, m), 730 (N-H, m). See Supplementary Figures S10-S12 for corresponding full spectra.

Brush synthesis and functionalisation

Polymer brushes were generated using a previously published method.[45, 46] Silicon wafer substrates were functionalised with an ATRP initiator using the following method: the substrates were plasma oxidised for 10 minutes (Zepto plasma cleaner, Henniker Scientific, power 95) and incubated in a solution of anhydrous toluene (30 mL) with 3-trimethoxysilyl

propyl 2-bromo-2 methylpropionate (30 µL) and triethylamine (50 µL) for 24 h. Substrates were washed with deionised water followed by ethanol and dried under a stream of nitrogen.

POEGMA-OH Brushes were then grown from the surface of the resulting silicon substrates functionalised with ATRP initiators. Poly ethylene glycol (PEG) methacrylate (hydroxyl terminated, 17.5 mmol), bipyridine (1.0 mmol), Cu (II) Br_2 (40 µmol) and water: ethanol 4:1 (12:3 mL) were added to a round bottom. The solution was bubbled with argon for 45 minutes whilst stirring. Then was added Cu (I) Cl (410 µmol), the contents were sonicated and bubbled with argon for a further 10 minutes. The polymerisation solution was transferred to reaction tubes containing substrates, under inert atmosphere, in order to initiate the polymer brush growth. Polymerisations were stopped by opening reaction mixtures to air and adding copious amount of water. Substrates were washed with plenty of water then ethanol and dried under a stream of nitrogen. The thickness of the resulting brushes was measured using ellipsometry.

For the functionalisation of POEGMA-OH brushes, terminal hydroxyl groups were functionalised via DSC coupling. Brushes were functionalised with a solution of DSC (60 mmol) and DMAP (60 mmol) in anhydrous DMF (60 mL), under inert atmosphere for 24 h. Substrates were washed with DMF followed by water and ethanol and dried under a stream of nitrogen. The thickness of the resulting brushes was measured via ellipsometry. DSC activated brushes were then functionalised with alkenes. The DSC functionalised brushes were incubated in a solution of 1 % allylamine in DMF (10 µL/mL) or 1 % norbornene in PBS (10 mg/mL) for 24 h. The substrates were washed with DMF (for allylamine substrates only), water, ethanol and dried under a stream of nitrogen. The thickness of the resulting POEGMA-AA and POEGMA-NB brushes was measured via ellipsometry.

Methacrylate functionalised substrates

Silicon wafers were plasma oxidised for 10 min (Zepto plasma cleaner, Henniker Scientific, power 95) and incubated in a solution of anhydrous toluene (30 mL) with 3-(trimethoxysilyl)propyl methacrylate (30 µL) and triethylamine (50 µL) for 24 h. The wafer was washed with deionised water followed by ethanol and dried under a stream of nitrogen.

Thiol-ene coupling on polymer brush-functionalised substrates

A series of thiols (**T1**-**7**) were dissolved in PBS (45 µmol/mL) and thiol **S8** was dissolved in DMF: PBS (2: 8), due to its lower solubility. For UV-initiated reactions, the photoinitiator Irgacure 2959 (5 mol% with respect to the thiol, typically 25 µL/mL of 250 mg/mL solution in methanol) was added to the thiol solution. For visible light initiated reactions, Eosin Y (0.02 w/v%) and triethanolamine (0.2 v/v%) was added to the thiol solution. The mixture was added onto a quartz plate (10 µL) and alkene-functionalised brushes or methacrylate-functionalised substrates were placed on top, face down. Substrates were cured with UV (300 s, 17mW/cm^2) or visible light (300 s, 100mW/cm^2) as shown in setup (Figure S1 in Supporting Information). Substrates were washed with deionised water then ethanol and dried under a stream of nitrogen before characterisation via ellipsometry.

Cell culture and seeding onto substrates

HUVECs were routinely grown in medium 199 supplemented with 10 % FBS, 1 % penicillin streptomycin and 1 % glutamine. The medium was changed every 2-3 days and cells were sub-cultured each week using trypsin/versene. Cells were maintained at 37 ºC in a humidified atmosphere containing 5 % CO_2.

Cell adhesive control substrates coated with collagen were prepared according to the following protocol: collagen rat, type I was dissolved in PBS (400 µg/mL) and filtered through a 0.2 µm pore membrane. The collagen mixture was added to a well containing a coverslip and allowed

to set for 30 minutes. The solution was removed and replaced with PBS before cell seeding cells.

For polymer brush coated substrates: Thiol-ene functionalised substrates were sterilised with ethanol for 10 min and washed with sterile PBS. HUVECs at a passage 4-12 (15,000 cells/mL) in medium (1 mL) were seeded on the substrates and cultured for 24 h. Cells were fixed and permeabilised simultaneously in 4 % PFA and 0.2 % Triton-X100, blocked for 1 h in 10% FBS containing 0.25 % gelatine, incubated at room temperature with phalloidin (2 µL/mL) and DAPI (2 µL/mL) for 1 h and mounted on glass slides in Mowiol. Epifluorescence microscopy was used to image cells adhered to the surfaces and images were analyzed using image J.

Patterning of peptides on brushes

Patterned substrates were generated as for the homogeneous substrates (with N-acetyl L-cysteine **T1** and FITC RGE **T8**). Instead of adding the reaction mixture (containing 5 mol% of PI) to the quartz, it was added to the photomask (acetate mask for discs and lines patterns; chromium mask for rectangles and rings patterns) according to the setup depicted in Figure S7. Irradiation and washing were then carried out as for homogenous substrates. Substrates were imaged using epifluorescence microscopy and AFM.

Cell culture on patterned brushes

Patterned substrates were generated with 1:1 **T5**:**T8** mixed solutions. Thiol solutions with PI were used to generate ring patterns, as described above. After washing, substrates were sterilised with ethanol and sterile PBS. HUVECs (7,500 cells/mL) in medium (1 mL) were seeded on the substrates and cultured for 24 h. Patterned cells were fixed and permeabilised simultaneously in 4 % PFA and 0.2 % Triton-X100, blocked for 1 h in 10 % FBS containing 0.25 % gelatine, incubated at room temperature with phalloidin (2 µL/mL) and DAPI (2 µL/mL) for 1 h and mounted on glass slides in Mowiol. Epifluorescence microscopy was used to image cells adhered to the patterned surfaces.

Results and discussion

Thiol-ene coupling with POEGMA brushes

In order to confer specific controlled cell adhesion to polymer brushes, it is necessary to use protein resistant polymers that can prevent unwanted adsorption of ECM proteins, whilst enabling stable coupling of peptides promoting integrin binding. We selected POEGMA as the protein resistant brush, due to its control of protein adsorption, including from sera used in tissue culture such as foetal bovine serum.[9, 19] In addition, the availability of cheap hydroxyl-terminated OEGMA-OH monomers enables the simple introduction of functional moieties to promote coupling via thiol-ene chemistry. Hence discuccinimidyl carbonate (DSC) coupling, which has been shown to be particularly efficient in protein coupling to polymer brushes,[47] was used for the activation of brushes and reaction with small amino-alkenes (allylamine and norbornene derivative **1**, Figure 1 and Scheme 1). The thickness of POEGMA brushes can be readily controlled through the catalytic system used (e.g. nature of solvent and ligands) and the reaction time.[9] After 75 min polymerisation, pure POEGMA-OH brushes with a thickness of 40 nm were obtained, as determined by ellipsometry. AFM scans were performed in the dry and swollen state, and indicated a surface roughness 0.3 nm (Supplementary Information Figure S15). The resulting brushes were further functionalised with amines (allylamine and norbronene **1**), using DSC activation. Functionalisation was confirmed first by ellipsometry and the associated increase in brush height (although small considering the size of OEGMA monomers compared to the small molecules grafted), following protocols previously reported (see Figure S2 and equations S1 and S2 in Supporting Information).[35] AFM scans of POEGMA-AA brushes were compared to those of POEGMA-OH surfaces and indicated a roughness of 0.6 and 0.3 nm in the dry and swollen state, respectively (Supplementary Information Figure S15), indicating little changes in brush homogeneity upon functionalisation. Hence we achieved 20-30% functionalisation with allylamine and

norbronene **1**. Such values are in line with the moderate functionalisation levels typically achieved for polymer brushes, often restricted to the surface (upper layer) of the brush, due to limited diffusion.[35, 48] However surface functionalisation should be sufficient to promote cell adhesion, as integrins are not sought to be able to penetrate within the brush for binding with ligands, as indicated by previous studies that investigated the role of the localisation of integrin ligands within brushes.[36, 37]

We next examined the extent of radical-mediated thiol-ene coupling to the resulting alkene-functionalised POEGMA brushes. Indeed thiol-ene coupling should allow the immobilisation of biomolecules on the surface of polymeric brushes, as has been demonstrated for other biomaterials,[41, 42, 49, 50] and readily occurs at moderate concentrations, in buffers compatible with cell culture and the preservation of protein structures.[38] In particular, we aimed to promote coupling of cysteine residues within peptide sequences to anchor onto alkene functional POEGMA brushes. Alkene functionalised POEGMA brushes were reacted with a series of thiols (Table 1) upon irradiation with UV light, in the presence of the photoinitiator Irgacure 2959 (at different concentrations). N-Acetyl L-cysteine (**T1**) and L-glutathione (**T2**) were used as model thiols to study the efficiency of the reaction and to optimise the reaction conditions, with 2 mol % and 5 mol % photoinitiator (Irgacure 2959) with respect to the thiol, for varying times of UV irradiation (17 mW/cm^2, Figure 2). Ellipsometry results indicated that functionalisation levels reached a plateau after 30 s of irradiation (Figure 2A), in good agreement with kinetics observed for thiol-ene reactions on PGMA brushes.[35] An increase in the concentration of PI from 2 to 5 mol% increased the degree of functionalisation and conversions were higher for **T1** than for **T2**, presumably due to the larger size of **T2** and associated steric hindrance and reduced molecular diffusion through the brush, as was observed for PGMA brushes.[35] This was evidenced by characterising thiol-ene efficiencies for different brush thicknesses (as equations S1 and S2 make the assumption of homogenously distributed

substitution, Figure 2A). Little changes were observed in coupling efficiency at different brush length (Figure 2B), suggesting that, in addition to diffusion, competitive side-reactions may limit coupling to POEGMA brushes. Indeed, if molecular diffusion was solely responsible for limiting coupling efficiency, functionalisation levels should have decreased as brush thicknesses increased. In contrast, competitive radical coupling (for example crosslinking of brushes themselves) is expected to reduce overall thiol-ene coupling efficiencies. However, the occurrence of gradients in brush density along their depth profile, and the only partial alkenation of POEGMA-OH brushes, could also account for such observations. Overall, we determined that 300 s UV exposure and 5 mol% of photoinitiator would be suitable conditions for further studies of thiol-ene coupling of peptides to POEGMA brushes. In addition, we confirmed that control reactions carried out in the presence of **T5** and with UV irradiation, but without any photoinitaor, did not result in increases in brush thickness. Hence, the coupling of peptides specifically occured via thiol-ene reaction, in the presense of photoinitiator.

As the swelling of brushes could potentially affect the displacement effectively sensed by cells spreading on these coatings (with a critical length scale between 40 and 200 nm)[51], and be indicative of differences in crosslinking of the brushes used (and therefore their stiffness, affecting cell spreading)[52], we characterised the swelling of functionalised brushes via in situ ellipsometry (Supplementary Information Figure S16). Results indicate very limited swelling levels for all brushes, in line with previous reports[25, 53, 54], due to the presence of dimethacrylate monomers in the OEGMA-OH monomer supplied by Sigma. The limited difference in swelling even after functionalisation (between 15 and 60 %, corresponding to distances below 20 nm) is therefore indicating that cells should not be able to sense changes in brush swelling due to slight differences in functionalisation chemistry (e.g. changes in amino acid sequence).

Results show an inscrease in the brush swelling when functionalised with either allylamine or norbornene. Allylamine brushes functionalised with acetyl cysteine showed further swelling.

The functionalization of brushes plays a role in the swelling behaviour, this may be related to the wettability of the surface.

Grazing angle FTIR was used to further confirm the functionalisation of POEGMA brushes with allylamine and thiols **T1** and **T2** (Figure 3). The broad band at 3300-3600 cm^{-1} corresponding to terminal hydroxyl groups (O-H symmetric stretch) of POEGMA brushes disappeared upon functionalisation with allylamine.[55] Carbonyl bands (C=O symmetric stretch) at 1730 cm^{-1} and alkane peaks (C-H symmetric stretch) at 2860-2960 cm^{-1} were present for all samples, as expected from the corresponding structures. New bands at 1530 cm^{-1} (C-N stretch and N-H bend) and 1650 cm^{-1} (C=O amide I band) appeared after functionalisation of POEGMA with allylamine and thiols **T1**, **T2** and **T5** (see discussion below for the coupling of **T5**). The 1650 cm^{-1} shoulder, assigned to amide I vibrations, also became more intense after functionalisation of allylamine residues with the thiols, as expected from the corresponding amino acid and peptidic backbones of the corresponding thiols. Hence, overall our results confirm the successful functionalisation of POEGMA brushes via thiol-ene chemistry.

Norbornene moieties display particularly reactive alkenes due to the degree of strain of this bicyclic molecule. Hence norbornene derivatives have been extensively used in metathesis and radical reactions.[56-59] Therefore, we next examined the use of norbornene-functionalised brushes to promote the coupling of thiols via a radical mechanism. The coupling of **T1** to norbornene and allylamine brushes was compared first (Figure S3 in Supporting Information). Surprisingly, norbornene moieties were found to sustain lower coupling efficiencies to POEGMA brushes compared to allylamine residues. However, this could be the result of the lower functionalisation level achieved with norbronene, compared to allylamine, or differences in the hydrophilicity of norbronene residues. In addition, recent reports have indicated that norbornene moieties are suitable for activation using Eosin Y and triethanol amine as the radical initiator, upon irradiation with visible light (in the range of 400-700 nm).[59-61] Hence we

compared thiol-ene coupling under UV and visible light irradiation, in the presence of Irgacure 2959 and Eosin Y, respectively. With 300 s exposure, the coupling efficiencies of **T1** to POEGMA-AA and POEGMA-NB decreased from 51 % and 36 % (respectively), under UV irradiation, to 4 % and 8 % (respectively), under visible light irradiation. Therefore, although norbornene was slightly more efficient under visible light irradiation (with Eosin Y), coupling efficiencies remained relatively low, even for a small molecule such as **T1**.

Subsequently, the coupling of cysteine-bearing peptides (Table 1) was quantified, to determine the impact of molecular size on thiol-ene efficiency. These sequences were selected based on their ability to promote cell adhesion (and associated negative controls), mimicking binding to different ECM proteins.[62, 63] Reaction efficiencies for the coupling of **T3-8** to POEGMA-AA brushes are presented in Figure 2C. Compared to smaller **T1** and **T2** thiols, reaction efficiencies decreased significantly with increasing molecular weight (down to 6 to 11 %), presumably due to the steric hindrance associated with the size of these molecules and the high density of the polymer brushes used, restricting molecular diffusion. All peptides displayed relatively comparable coupling efficiencies, however GCGREDVSG displayed perhaps slightly higher couplings (11 %), compared to GCGPHSRNSG (3 %). This may be due to differences in amino acid composition, which may result in differences in peptide conformation as well as changes in local pH environments near the reactive cysteines.[38]

To further confirm the successful peptide functionalisation of POEGMA brushes via thiol-ene coupling, XPS spectra were recorded for POEGMA brushes at different stages of functionalisation (Figure S14 in Supplementary Information and Table 2). As expected, the XPS spectrum of unfunctionalised POEGMA brushes displayed oxygen and carbon peaks only. After activation with disuccinimidyl carbonate, 1.6 atom % of nitrogen appeared and this increases to 1.8 atom % after reaction with allylamine. In addition, a new peak appeared in the C spectrum at 290.3 eV, associated with carbonate groups[53]. When POEGMA-DSC brushes

were functionalised with norbornene **1**, an increase in the peak intensity at 284 eV was observed, confirming the increase in alkyl group content. After functionalization of POEGMA-AA or POEGMA-NB brushes via thiol-ene chemistry, an increase in the nitrogen content was observed, associated with the addition of peptide side chains (**T1**, **T5**). The increase in % atom of nitrogen reflects the number of nitrogen atoms in the coupled molecules (higher for **T5** than **T1**). Finally, after thiol-ene coupling, a new peak appeared in the spectra, associated with the presence of sulphur (0.5-1.1 atom %), in agreement with the thio ether formed.

Cell adhesion to functionalised polymer brushes

The immobilisation of biomolecules on polymer brushes and the regulation of cell behaviour that such platforms allow is of particular interest for the design of cell-based assays.[14, 31, 64] However the control of cell patterning directly with light has remained difficult. Such direct activation of surfaces and the spatial control that it permits would be particularly attractive for the *in situ* control of cell spreading and migration.[14, 65, 66] In order to establish whether thiol-ene coupling is suitable for the patterning of cells and the design of cell-based assays, we studied the specificity with which cell adhesion can be controlled upon functionalisation of POEGMA brushes. In particular, we examined the specificity of the surfaces generated, to promote cell adhesion via binding of the selected peptides.

To test the cell resistance of functionalised POEGMA brushes, human umbilical vein endothelial cells (HUVECs) were seeded onto POEGMA-coated substrates functionalised with allylamine and norbornene. Cells were allowed to spread for 24 h, fixed and stained, the number of cells adhered and their areas were characterised (Figure S4 in Supporting Information). POEGMA-OH and POEGMA-AA brushes displayed low cell adhesion (although slightly higher in the case of allylamine-funcationalised brushes, perhaps due to a slight increase in hydrophobicity of some of the side groups and the presence of proton donors and acceptors in the new structures formed) and the cells that managed to adhere remained relatively rounded.

In comparison, significantly higher densities of cells adhered to POEGMA-NB and managed to spread to higher extents. Therefore our results indicate that the introduction of norbornene moieties in POEGMA-NB brushes gives rise to significant cell fouling, presumably because of the hydrophobic character of this residue. We attempted to decrease the content of POEGMA-OH (and therefore Norbornene residues) within the brush (with methoxy-capped OEGMA monomers), but this did not completely prevent cell aldhesion and spreading (results not shown). Hence POEGMA-AA brushes were selected for further study cell adhesion specificity to peptides **T3**-**T6**.

We next studied the role of functionalisation with peptides that specifically promote binding of integrins in order to establish the specificity of the bioactive POEGMA brushes designed. In addition, we proposed to explore using our platform the role of $\alpha_5\beta_1$, $\alpha_v\beta_3$ and $\alpha_4\beta_1$ integrins in the establishment of HUVEC spreading. HUVECs were seeded on POEGMA brushes functionalised with peptides **T3-T6** and their adhesion and spreading was monitored after 24 h and compared to collagen-coated substrates and non-functionalised POEGMA and POEGMA-AA brushes (Figure 4 and S5). Cell adhesion and spreading was found to be comparable on RGD-functionalised brushes and collagen controls, in agreement with the importance of this peptide in the binding of $\alpha_5\beta_1$ and $\alpha_v\beta_3$ integrins, expressed by HUVECs.[62, 67, 68] In contrast, cell densities remained low and spreading was impaired on non-functionalised POEGMA and POEGMA-AA brushes as well as RGE functionalised brushes. Interestingly, REDV functionalised brushes did not enable cell adhesion or spreading, in contrast to reports implying their activity to promote HUVECs spreading.[63, 64] Therefore our results imply that $\alpha_4\beta_1$ integrin, binding to the REDV sequence, [63, 64, 69, 70] is insufficient, on its own, to support HUVECs adhesion and spreading. To further confirm the specificity of our brush-based platform, we functionalised methacrylate monolayers with peptides **T3**-**T6** and studied HUVECs adhesion via immunostaining after 24 h of culture (Figure 6 in Supporting Information). Cell densities

and spreading were relatively comparable on all substrates, indicating the importance of maintaining a robust anti-fouling background to study the specificity of peptide binding. Therefore our platform appears particularly well suited for the systematic design of peptides selectively engaging cell membrane receptors and their impact on cell spreading and motility.

Patterning peptides on brushes

Cells are sensitive to geometrical and mechanical constraints from their environment *in vivo*.[7] These factors are not controlled under classic culture conditions. The ability to confine cells to specific microenvironments and the effect of such cues on cell behaviour has been used to design cell-based assays aimed at probing molecular mechanisms regulating cell phenotype.[15, 16, 71] Cell patterning has been used to control the geometry and size of cells and help to understand cell response to geometry of the extra-cellular environment. Photo-patterning provides an excellent tool for this purpose and thiol-ene coupling offers a simple method to control such chemical patterns. We therefore applied thiol-ene coupling to create various patterned surfaces, using a model FITC labelled peptide (**T8**) to characterise the quality of the patterns generated. For this purpose, we used the methodology used for direct irradiation of homogenous brushes, with the addition of a photomask to the system (Figure S7 in Supporting Information).

Following irradiation through photomasks (50 µm circles and 50 µm lines), the patterning quality of the peptides coupled to POEGMA-AA brushes was characterised by epifluorescence microscopy (Figure 5). Clear peptide patterns were observed with good reproduction of the original photomasks and dimensions of the patterns, and high contrast between background and patterned areas. A slight broadening of the features was observed (approximately 10%), which may result from the low resolution of the acetate masks used and its lack of contact with the brush, therefore enabling diffraction of light during irradiation. The impact of patterning conditions on coupling efficiency and pattern definition was assessed next. Substrates were

reacted for different UV exposure times (60, 180, 300s UV). The corresponding epifluorescence images and analysis are presented in Figure S8 (Supporting Information). Although the pattern intensity was strongly affected by the exposure time, we observed limited changes in the pattern dimension and broadening of the features, suggesting limited contribution of diffusions of thiyl radicals whithin the solutions exposed.

In order to characterise the definition of the patterns at a higher resolution, via atomic force microscopy, we used patterns with smaller feature sizes (10 by 2 μm dark rectangles) and characterised the resolution of the patterns after different UV exposure times (60, 180,300 s UV, using **T1** and **T8**). Epifluorescence images and analysis of **T8**-functionalised patterns are presented in Figures 5 and S9 (Supporting Information). As for larger patterns, increasing peptide densities were observed with increasing UV exposure times. AFM was used to characterise the topography of **T1**-functionalised patterns, which was expected to result from the increase in brush thickness in the functionalised areas (Figures 5 and S9). Clear rectangular patterns can be observed via AFM and contour profiles were analysed to characterise the pattern definition and the increase in UV exposure times (up to 300 s UV exposure) improved the definition of the patterns, as established by the slope of the transition areas (0.6, 1.0 and 1.5 nm/μm, for 60, 180 and 300 s irradiation, respectively), confirming the results obtained by fluorescence microscopy for larger patterns (50 μm). However this increase in the sharpness of the contour is associated with an increase in overall brush height in non-irradiated area, suggesting some level of scattering, in agreement with the overall higher intensity of the non-patterned areas observed by fluorescence microscopy (Figure 5E). Overall, our results indicate that thiol-ene coupling is well-suited for the generation of peptide patterns at the surface of polymer brushes, but that optimisation of the irradiation conditions, together with the resolution and configuration of the photomask used, are essential to achieve high patterning fidelity.

Cell interaction with thiol-ene patterned brushes

We next studied cell patterning using our thiol-ene mediated peptide-functionalised brushes. Indeed, the design of cellular patterns in which cell shape and spreading are controlled plays an important role in the development of cell-based assays.[15, 16, 71] Based on our cell adhesion data (Figure 4), the RGD peptide **T5** was selected, due to its specific control of cell adhesion and spreading. To enable visualisation of the patterns, polymer brushes were functionalised with a mixture of **T5** and **T8** (1:1), using masks displaying 50 µm rings that were previously used to study the role of cell membrane interactions with polymer brushes presenting different chemistries.[25] Here too, POEGMA-AA brushes were selected for their antifouling properties, compared to POEGMA-NB brushes and the quality of cell arrays obtained after incubation of HUVECs for 24 h was examined via epifluorescence microscopy (Figure 6). Cells adhered to the adhesive rings presented by the peptides and formed ordered patterns matching those defined by the photomask used. Hence our results demonstrate the potential of photoinitiated thiol-ene coupling for the patterning of polymer brushes and the generation of cell arrays that can be used for the control of the cell microenvironment in cell-based assays (peptide chemistry and composition as well as pattern size and shape).

Conclusion

Considering the ease with which cysteins can be introduced in peptide structures, thiol-ene chemistry provides an excellent tool for the biofunctionalisation of polymeric surfaces and the generation of micropatterns of defined size and shape. Our results demonstrated the quality of the peptide arrays generated using this approach, and their ability to control cellular patterning. In addition, antifouling POEGMA brushes appear particularly well-suited for the control of cell adhesion to specific peptide sequences, therefore paving the way to studies investigating the structure-property relationships connecting peptide sequences and integrin (or other membrane receptor) binding. This will allow, for example, the study of the impact of specific

integrin binding (controlled via the choice of peptides coupled) on the sensing of the ECM geometry, which has been shown to regulate the axis of cell division and to direct the differentiation of stem cells. In particular, such patterned polymer brushes are well-suited for high-throughput and high content screens and the formation of substrate libraries that can be used for the study of molecular pathways and signalling mechanisms regulating cell phenotype. Finally, beyond cellular assays, the ability to immobilise bioactive peptides with high selectivity on antifouling coatings is also of particular interest for the design of biosensors.

Associated content

Supporting Information. Characterisation of norbornene **1**, ellipsometry, XPS and AFM characterisation of brush functionalisation, characterisation of cell adhesion and substrate patterning and associated epifluorescence microscopy images and statistical analysis.

Author Information

Corresponding Author.
*E-mail: j.gautrot@qmul.ac.uk.
ORCID.
Julien E. Gautrot: 0000-0002-1614-2578.
Notes.
The authors declare no competing financial interest.

Acknowledgment

B.C. and S.D.C thank Queen Mary, University of London and the Institute of Bioengineering for their PhD studentships. Funding from the Royal Society (RG110425) to support consumables and reagents is acknowledged.

References

(1) Stuart, M. A. C.; Huck, W. T. S.; Genzer, J.; Mueller, M.; Ober, C.; Stamm, M.; Sukhorukov, G. B.; Szleifer, I.; Tsukruk, V. V.; Urban, M.; Winnik, F.; Zauscher, S.; Luzinov, I.; Minko, S., *Nat. Mater.* **2010,** *9* (2), 101-113.

(2) Liu, M.; Jiang, L., *Adv. Funct. Mater.* **2010,** *20* (21), 3753-3764.

(3) Hucknall, A.; Rangarajan, S.; Chilkoti, A., *Adv. Mater.* **2009,** *21* (23), 2441-2446.

(4) Alf, M. E.; Asatekin, A.; Barr, M. C.; Baxamusa, S. H.; Chelawat, H.; Ozaydin-Ince, G.; Petruczok, C. D.; Sreenivasan, R.; Tenhaeff, W. E.; Trujillo, N. J.; Vaddiraju, S.; Xu, J.; Gleason, K. K., *Adv. Mater.* **2010,** *22* (18), 1993-2027.

(5) Azzaroni, O., *J. Polym. Sci., A: Polym. Chem.* **2012,** *50*, 3225-3258.

(6) Barbey, R.; Lavanant, L.; Paripovic, D.; Schuwer, N.; Sugnaux, C.; Tugulu, S.; Klok, H.-A., *Chem. Rev.* **2009,** *109*, 5437-5527.

(7) Thery, M., *J. Cell Sci.* **2010,** *123* (24), 4201-4212.

(8) Thery, M.; Racine, V.; Piel, M.; Pepin, A.; Dimitrov, A.; Chen, Y.; Sibarita, J.-B.; Bornens, M., *Proc. Natl. Acad. Sci.* **2006,** *103* (52), 19771-19776.

(9) Gautrot, J. E.; Trappmann, B.; Oceguera-Yanez, F.; Connelly, J.; He, X.; Watt, F. M.; Huck, W. T. S., *Biomaterials* **2010,** *31*, 5030-5041.

(10) Gautrot, J. E.; Wang, C.; Liu, X.; Goldie, S. J.; Trappmann, B.; Huck, W. T. S.; Watt, F. M., *Biomaterials* ***2012*****,** *33* (21), 5221-5229.

(11) Kilian, K. A.; Bugarija, B.; Lahn, B. T.; Mrksich, M., *Proc. Natl. Acad. Sci.* **2010,** *107* (11), 4872-4877.

(12) Salierno, M. J.; Garcia, A. J.; del Campo, A., *Adv. Funct. Mater.* **2013,** *23*, 5974-5980.

(13) Kamimura, M.; Sugawara, M.; Yamamoto, S.; Yamaguchi, K.; Nakanishi, J., *Biomater. Sci.* **2016,** *4*, 933-937.

(14) Costa, P.; Gautrot, J. E.; Connelly, J., *Acta Biomater* **2014,** *10* (6), 2415-2422.

(15) McBeath, R.; Pirone, D. M.; Nelson, C. M.; Bhadriraju, K.; Chen, C. S., *Dev. Cell* **2004,** *6*, 483-495.

(16) Connelly, J.; Gautrot, J. E.; Trappmann, B.; Tan, D. W. M.; Donati, G.; Huck, W. T. S.; Watt, F. M., *Nat. Cell Biol.* **2010,** *12*, 711-718.

(17) Becker, A. L.; Henzler, K.; Welsch, N.; Ballauff, M.; Borisov, O., *Curr. Opin. Coll. Interf. Sci.* **2012,** *17*, 90-96.

(18) Sakata, S.; Inoue, Y.; Ishihara, K., *Langmuir* **2014,** *30*, 2745-2751.

(19) Ma, H.; Hyun, J.; Stiller, P.; Chilkoti, A., *Adv. Mater.* **2004,** *16* (4), 338-341.

(20) Ladd, J.; Zhang, Z.; Chen, S.; Hower, J. C.; Jiang, S., *Biomacromolecules* **2008,** *9* (5), 1357-1361.

(21) Vaisocherova, H.; Yang, W.; Zhang, Z.; Cao, Z.; Cheng, G.; Piliarik, M.; Homola, J.; Jiang, S., *Anal. Chem.* **2008,** *80* (20), 7894-7901.

(22) Yang, W.; Xue, H.; Li, W.; Zhang, J.; Jiang, S., *Langmuir* **2009,** *25* (19), 11911-11916.

(23) Rodriguez-Emmenegger, C.; Brynda, E.; Riedel, T.; Houska, M.; Subr, V.; Alles, A. B.; Hasan, E.; Gautrot, J. E.; Huck, W. T. S., *Macromol. Rapid Commun.* **2011,** *32*, 952-957.

(24) di Cio, S.; Boggild, T. M. L.; Connelly, J.; Sutherland, D. S.; Gautrot, J. E., *Acta Biomater* **2017,** *50*, 280-292.

(25) Tan, K. Y.; Lin, H.; Ramstedt, M.; Watt, F. M.; Huck, W. T. S.; Gautrot, J. E., *Integr. Biol.* **2013,** *5*, 899-910.

(26) Becker, A. L.; Welsch, N.; Schneider, C.; Ballauff, M., *Biomacromolecules* **2011,** *12*, 3936-3944.
(27) Haupt, B.; Neumann, R.; Wittemann, A.; Ballauff, M., *Biomacromolecules* **2005,** *6*, 948-955.
(28) Henzler, K.; Haupt, B.; Ballauff, M., *Anal. Biochem.* **2008,** *378*, 184-189.
(29) Riedel, T.; Rodriguez-Emmenegger, C.; de los Santos Pereira, A.; Bedajankova, A.; Jinoch, P.; Boltovets, P. M.; Brynda, E., *Biosens. Bioelectron.* **2014,** *55*, 278-284.
(30) Vaisocherova, H.; Sevcu, V.; Adam, P.; Spackova, B.; Hegnerova, K.; de los Santos Pereira, A.; Rodriguez-Emmenegger, C.; Riedel, T.; Houska, M.; Brynda, E.; Homola, J., *Biosens. Bioelectron.* **2014,** *51*, 150-157.
(31) Tugulu, S.; Silacci, P.; Stergiopulos, N.; Klok, H.-A., *Biomaterials* **2007,** *28*, 2536-2546.
(32) Glinel, K.; Jonas, A. M.; Jouenne, T.; Leprince, J.; Galas, L.; Huck, W. T. S., *Bioconj. Chem.* **2009,** *20*, 71-77.
(33) Gao, G.; Yu, K.; Kindrachuk, J.; Brooks, D. E.; Hancock, R. E.; Kizhakkedathu, J. N., *Biomacromolecules* **2011,** *12*, 3715-3727.
(34) Rodda, A. E.; Ercole, F.; Glattauer, V.; Nisbet, D. R.; Healy, K. E.; Dove, A. P.; Meagher, L.; Forsythe, J. S., *J. Mater. Chem. B* **2016,** *4*, 7314-7322.
(35) Tan, K. Y.; Ramstedt, M.; Colak, B.; Huck, W. T. S.; Gautrot, J. E., *Polym. Chem.* **2016,** *7*, 979-990.
(36) Desseaux, S.; Klok, H. A., *Biomaterials* **2015,** *44*, 24-35.
(37) Navarro, M.; Benetti, E. M.; Zapotoczny, S.; Planell, J. A.; Vancso, G. J., *Langmuir* **2008,** *24*, 10996-11002.
(38) Colak, B.; Da Silva, J. C. S.; Soares, T. A.; Gautrot, J. E., *Bioconj. Chem.* **2016,** *27* (9), 2111-2123.
(39) Gramlich, W. M.; Kim, I. L.; Burdick, J. A., *Biomaterials* **2013,** *34*, 9803-9811.
(40) Toepke, M. W.; Impellitteri, N. A.; Theisen, J. M.; Murphy, W. L., *Macromol. Mater. Eng.* **2013,** *298*, 699-703.
(41) Farrugia, B. L.; Kempe, K.; Schubert, U. S.; Hoogenboom, R.; Dargaville, T. R., *Biomacromolecules* **2013,** *14*, 2724-2732.
(42) Khetan, S.; Katz, J. S.; Burdick, J. A., *Soft Matter* **2009,** *5*, 1601-1606.
(43) Fittkau, M. H.; Zilla, P.; Bezuidenhout, D.; Lutolf, M.; Human, P.; Hubbell, J. A.; Davies, N., *Biomaterials* **2005,** *26* (2), 167-174.
(44) Blin, T.; Purohit, V.; Leprince, J.; Jouenne, T.; Glinel, K., *Biomacromolecules* **2011,** *12* (4), 1259-1264.
(45) Trmcic-Cvitas, J.; Hasan, E.; Ramstedt, M.; Li, X.; Cooper, M. A.; Abell, C.; Huck, W. T. S.; Gautrot, J. E., *Biomacromolecules* **2009,** *10* (10), 2885-2894.
(46) Brown, A. A.; Khan, N. S.; Steinbock, L.; Huck, W. T. S., *European Polymer Journal* **2005,** *41* (8), 1757-1765.
(47) Trmcic-Cvita, J.; Hasan, E.; Ramstedt, M.; Li, X.; Cooper, M.; Abel, C.; Huck, W. T. S.; Gautrot, J. E., *Biomacromolecules* **2009,** *10*, 2885-2894.
(48) Schuwer, N.; Geue, T.; Hinestrosa, J. P.; Klok, H.-A., *Macromolecules* **2011,** *44*, 6868-6874.
(49) Dargaville, T. R.; Forster, R.; Farrugia, B. L.; Kempe, K.; Voorhaar, L.; Schubert, U. S.; Hoogenboom, R., *Macromol. Rapid Commun.* **2012,** *33*, 1695-1700.
(50) Marklein, R. A.; Burdick, J. A., *Soft Matter* **2010,** *6*, 136-143.
(51) Attwood, S. J.; Cortes, E.; Haining, A. W. M.; Robinson, B.; Li, D.; Gautrot, J. E.; del Rio Hernandez, A., *Sci. Rep.* **2016,** *6*, 34334.
(52) Lilge, I.; Schonherr, H., *Angew. Chem., Int. Ed.* **2016,** *55*, 13114-13117.

(53) Gautrot, J. E.; Huck, W. T. S.; Welch, M.; Ramstedt, M., *Appl. Mater. Interfaces* **2010,** *51*, 193-202.
(54) Hackett, A. J.; Malmström, J.; Molino, P. J.; Gautrot, J. E.; Zhang, H.; Higgins, M. J.; Wallace, G. G.; Williams, D. E.; Travas-Sejdic, J., *J. Mater. Chem. B* **2015,** *3*, 9285-9294.
(55) Stuart, B., *Infrared Spectroscopy: Fundamentals and Applications*. 2004.
(56) Bielawski, C. W.; Grubbs, R. H., *Prog. Polym. Sci.* **2007,** *32*, 1-29.
(57) Blackwell, H. E.; Sadowsky, J. D.; Howard, R. J.; Sampson, J. N.; Chao, J. A.; Steinmetz, W. E.; O'Leary, D. J.; Grubbs, R. H., *J. Org. Chem.* **2001,** *66*, 5291-5302.
(58) Fairbanks, B. D.; Love, D. M.; Bowman, C. N., *Macromol. Chem. Phys.* **2017,** *218*, 1700073.
(59) Shih, H.; Liu, H.-Y.; Lin, C.-C., *Biomater. Sci.* **2017,** *5*, 589-599.
(60) Fu, A.; Gwon, K.; Kim, M.; Tae, G.; Kornfield, J. A., *Biomacromolecules* **2015,** *16*, 497-506.
(61) Shih, H.; Fraser, A. K.; Lin, C.-C., *Appl. Mater. Interfaces* **2013,** *5* (5), 1673-1680.
(62) Eisenberg, J. L.; Piper, J. L.; Mrksich, M., *Langmuir* **2009,** *25* (24), 13942-13951.
(63) Massia, S. P.; Hubbell, J. A., *J. Biol. Chem.* **1992,** *267* (20), 14019-14026.
(64) Monchaux, E.; Vermette, P., *Biomacromolecules* **2007,** *8* (11), 3668-3673.
(65) Jiang, X.; Bruzewicz, D. A.; Wong, A. P.; Piel, M.; Whitesides, G. M., *Proc. Natl. Acad. Sci.* **2005,** *102* (4), 975-978.
(66) van Dongen, S. F. M.; Maiuri, P.; Marie, E.; Tribet, C.; Piel, M., *Adv. Mater.* **2013,** *25*, 1687-1691.
(67) Chen, J.; Maeda, T.; Sekiguchi, K.; Sheppard, D., *Cell Adhes. Commun.* **1996,** *4* (4-5), 237-250.
(68) Houseman, B. T.; Mrksich, M., *Biomaterials* **2001,** *22*, 943-955.
(69) Seeto, W. J.; Tian, Y.; Lipke, E. A., *Acta. Biomater.* **2013,** *9* (9), 8279-8289.
(70) Plouffe, B. D.; Radisic, M.; Murthy, S. K., *Lab Chip* **2008,** *8* (3), 462-472.
(71) Connelly, J.; Mishra, A.; Gautrot, J. E.; Watt, F. M., *PLoS ONE* **2011,** *6* (11), e27259.

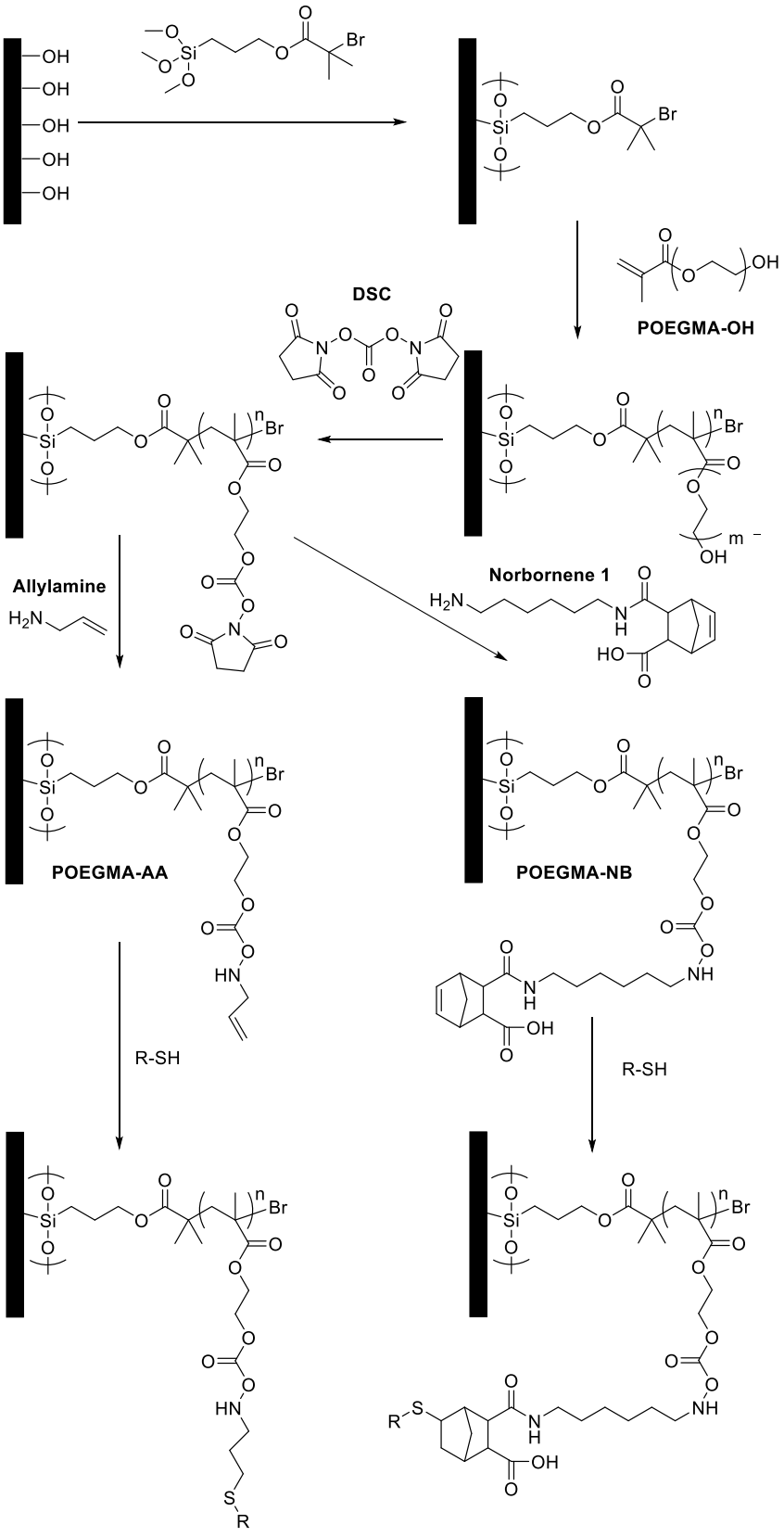

Scheme 1. Representation of POEGMA-OH brush synthesis, activation via DSC coupling and functionalisation with alkenese and thiol molecules.

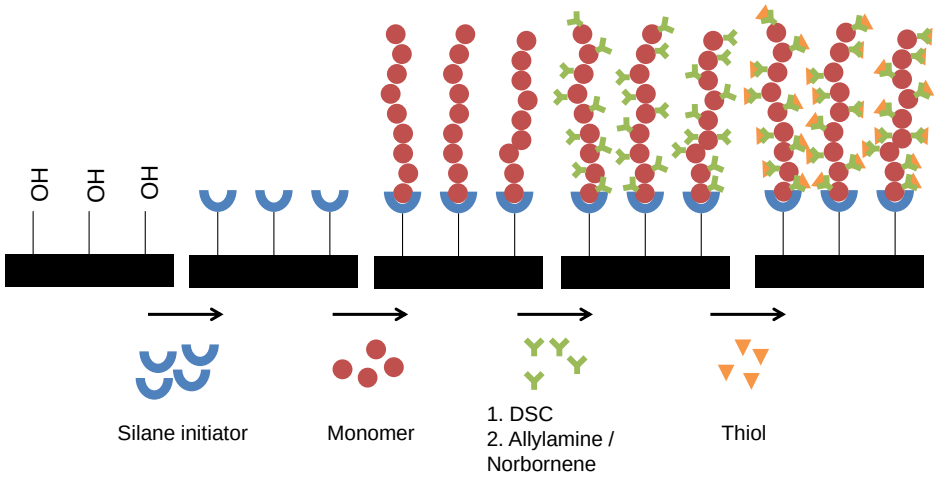

Figure 1. Successive steps involved in polymer brush formation and functionalisation via thiol-ene chemistry.

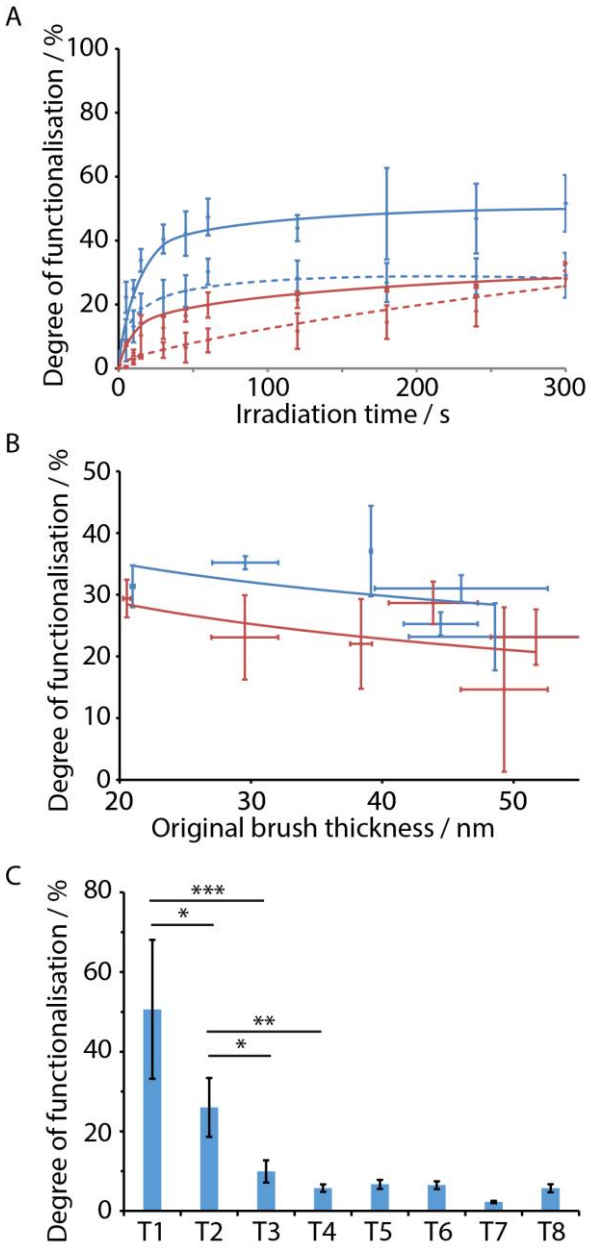

Figure 2. Thiol-ene functionalisation of POEGMA brushes. A. Effect of UV irradiation time and PI (Irgacure 2959) concentration on thiol-ene coupling efficiency (with thiols **T1**, blue lines, and **T2**, red lines; 5 mol% PI, dotted lines; 2 mol% PI; trendlines are only meant to guide the eye). B. Effect of POEGMA brush initial thickness (prior to functionalisation) on thiol-ene coupling, with 5 mol% PI, 300s UV irradiation time (blue, **T1** and red, **T2**; trendlines are only meant to guide the eye). C. Degree of functionalisation achieved for different thiols (**T1-8**) on POEGMA-AA (30-40 nm) surfaces with 5 mol% PI and 300 s UV exposure. See Supplementary Table S1 for corresponding statistical analysis.

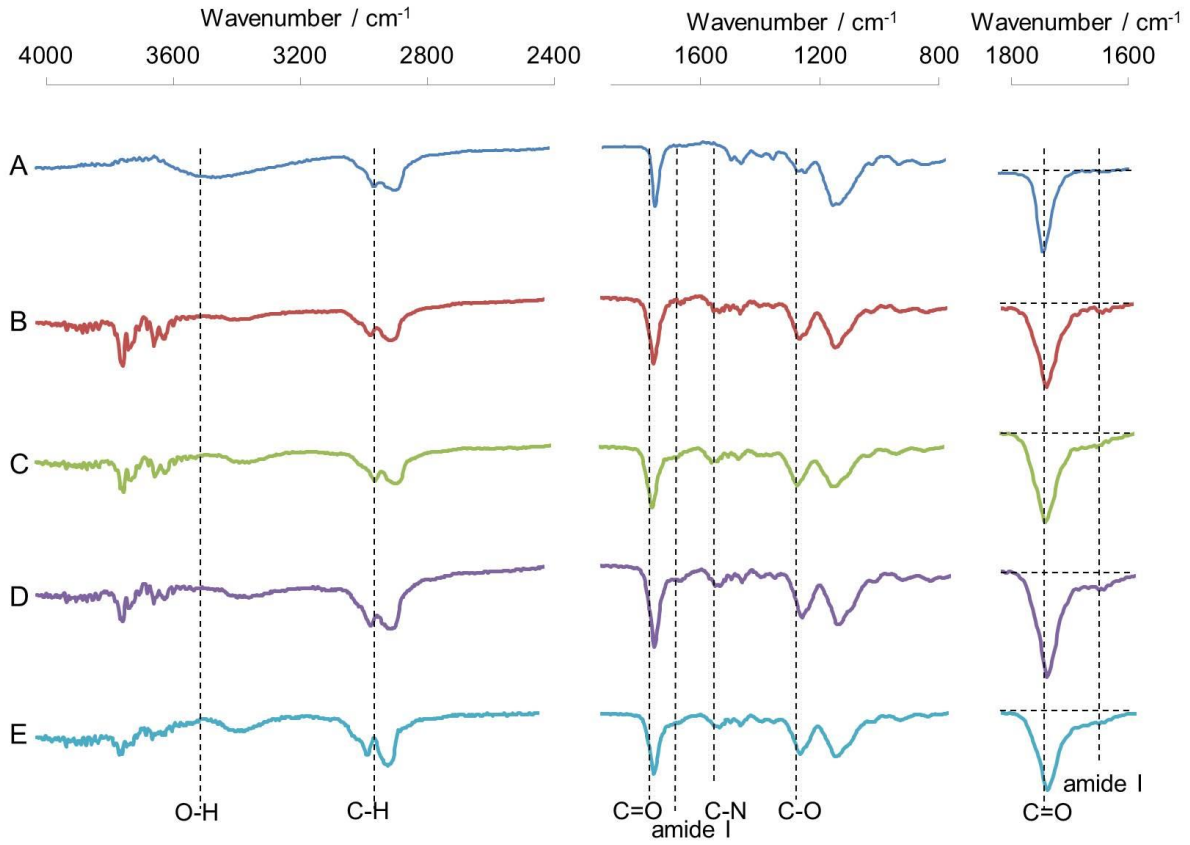

Figure 3. Grazing angle FTIR characterisation of functionalised POEGMA brushes: a) POEGMA, b) POEGMA-AA, c) **T1**-functionalised POEGMA-AA, d) **T2**-functioanlised POEGMA and e) **T5**-functionalised POEGMA. Thiol-ene coupling was carried out with 5 mol% PI and 300 s UV irradiation time.

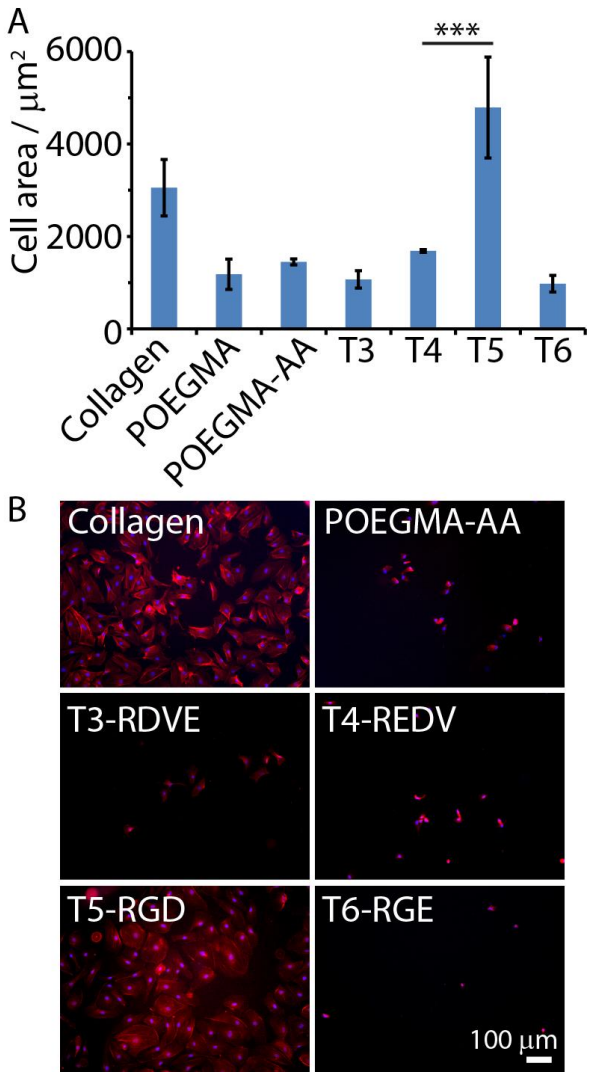

Figure 4. A. Spreading of HUVECs at the surface of peptide-functionalised POEGMA-AA brushes, with peptides **T3-6** (5 mol% PI, 300s UV) and collagen-coated glass as control. See Supplementary Table S5 for statistical analysis. B. Corresponding epifluorescence microscopy images (blue, DAPI; red, phalloidin).

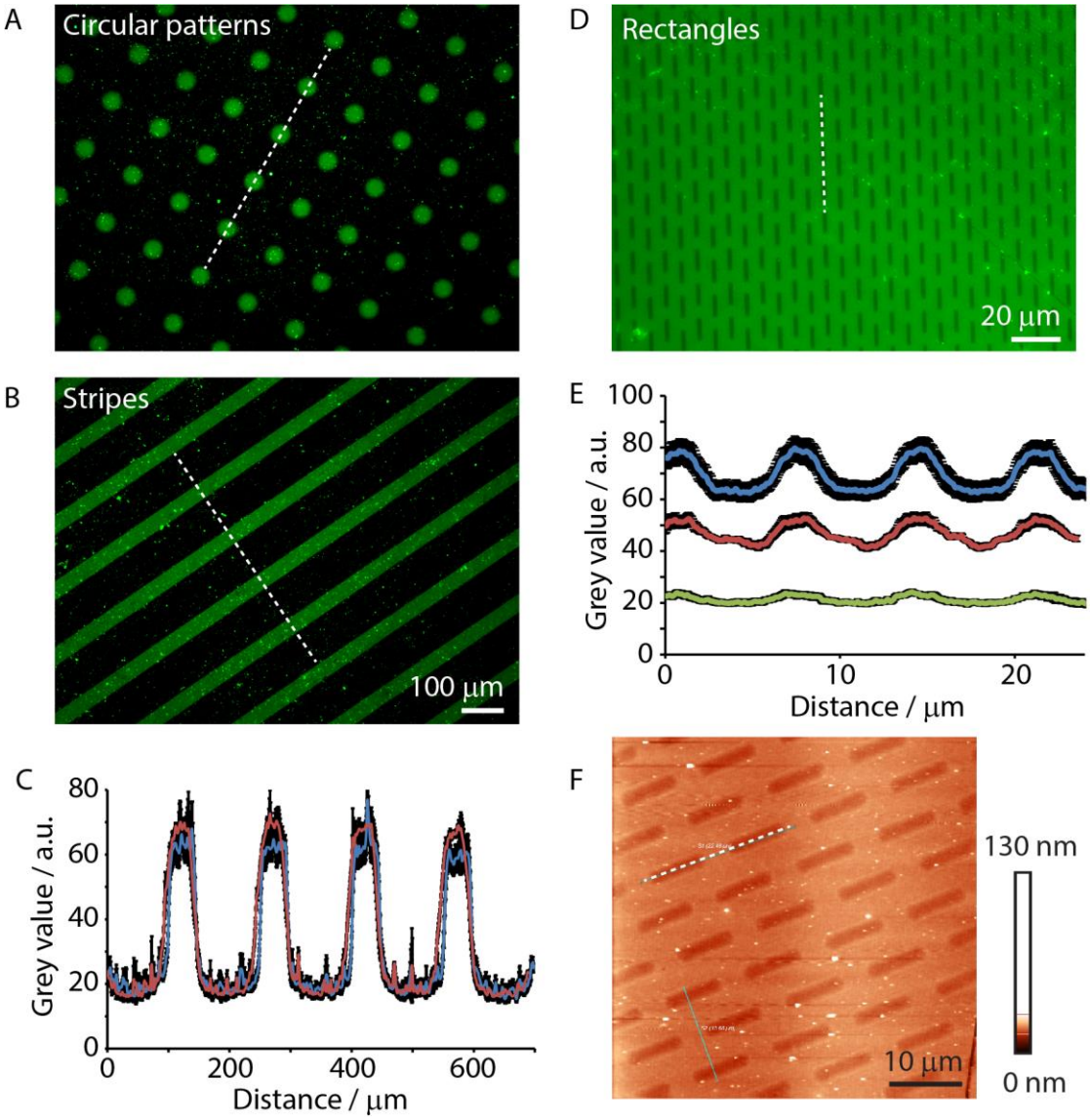

Figure 5. Micropatterning peptides to POEGMA-AA brushes via thiol-ene chemistry. A/B. Epifluorescence microscopy images of brushes patterned with FITC-RGE (**T8;** 50 µm circles and lines). C. Corresponding intensity profiles (in grey scale value; blue, circular patterns; red, lines) along dashed lines in A/B. Reactions were performed with 5 mol% PI and 300 s UV exposure. D. Smaller rectangular patterns of **T8** formed on POEGMA-AA brushes and corresponding intensity profiles (E, at different irradiation intensities, see Supplementary Figure S8 for images; blue, 300 s; red, 180 s; green, 60 s) and AFM characterisation (F, using **T1** instead of **T8**). Brush height profiles extracted from AFM images of patterns obtained at different irradiation times can be found in Supplementary Figure S9.

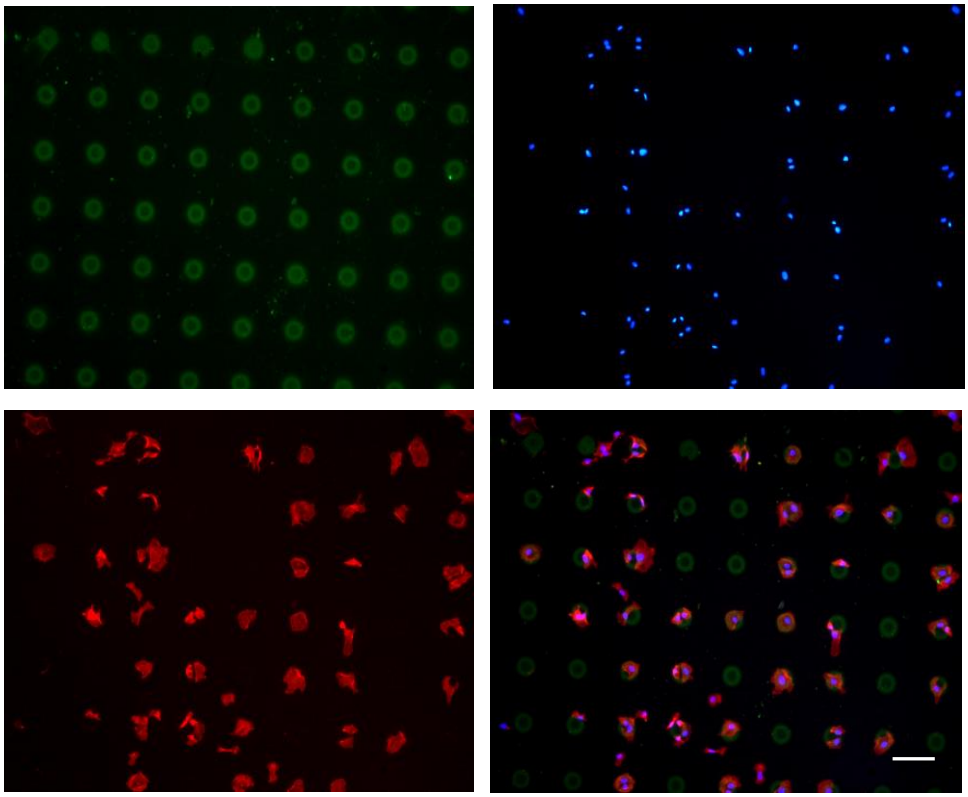

Figure 6. Microscopy images of HUVECs forming cell arrays at the surface of mixed peptide **T5** and **T8** (1/1 mole ratio) ring micropatterns (30 μm). Separate channels and merged images. Scale bar 100μm. Thiol-ene reactions for micropatterning were performed with 5 mol% PI and 300 s UV exposure. Green, RGE-FITC (**T8**); blue, DAPI; red, phalloidin.

Table 1. Series of thiols and peptides (**T1-8**) reacted with POEGMA-AA brushes using thiol-ene coupling.

Thiol	Sequence
T3	GCGREDVSG
T4	GCGRVDESG
T5	GCGYGRGDSPG
T6	GCGYGRGESPG
T7	GCGPHSRNSG
T8	GCGYGRGESPG-Lys-FITC-G

Table 2. Atom % composition of functionalised POEGMA brushes determined via XPS.

	C	**O**	**N**	**S**
POEGMA	70.1	29.9		
POEGMA-DSC	68.5	29.9	1.6	
POEGMA-AA	67.21	30.9	1.8	
POEGMA-NB	72.4	25.5	2.1	
POEGMA-AA-T1	68.0	28.6	2.3	1.1
POEGMA-AA-T5	70.4	22.5	6.6	0.5
POEGMA-NB-T1	71.5	25.2	2.5	0.7